2022

The Two-phase Flow Boiling Heat Transfer Coefficient of R448A Inside Multiport Mini-Channel Tube

Hieu Ngoc Hoang

Nurlaily Agustiarini

Jong-Taek Oh

The Two-phase Flow Boiling Heat Transfer Coefficient of R448A Inside Multiport Mini-Channel Tube

Hoang Ngoc HIEU[1]*, Nurlaily AGUSTIARINI[2], Jong-Taek OH[3]*

[1]Department of Refrigeration and Air-Conditioning, Graduate School, Chonnam National University, Yeosu, Chonnam, South Korea
206223@jnu.ac.kr

[2]Department of Refrigeration and Air-Conditioning, Graduate School, Chonnam National University, Yeosu, Chonnam, South Korea
208218@jnu.ac.kr

[3]Department of Refrigeration and Air-Conditioning, Chonnam National University, Yeosu, Chonnam, South Korea
ohjt@chonnam.ac.kr

* Corresponding Author

ABSTRACT

New regulations and restrictions against high GWP refrigerant have pressured the industry into adopting more environmentally friendly refrigerants. In this work, the heat transfer coefficient of a more recent zeotropic blend R448A inside multiport mini-channel tube was experimentally investigated. The mass flux range was from 100 to 500 kg/m^{2}s, heat flux from 3 to 15 kW/m^2, covering quality from 0 to 1 at fixed inlet temperature of 6°C and 3°C. It was found that the heat transfer coefficient increased with increased mass flux. Heat flux increased the heat transfer coefficient under low mass flux condition, while having no significant effect in high mass flux condition. A comparison was made between R448A and R410A inside a same test tube and it was found that R448A'S heat transfer coefficient was higher than R410A at low mass flux, but has similar order of magnitude in high mass flux conditions. Pressure drop of R448A increase with increased mass flux, and vapor quality, while heat flux displayed no significant effect on heat transfer coefficient. Finally, a simple heat transfer correlation was proposed for the practical prediction of R448A heat transfer coefficient within multiport mini-channel tube.

1. INTRODUCTION

Refrigeration and heat pump industry have to continuously undergo update to mitigate the field environmental impact. According to the EU Regulation No 517/2014, stationary refrigeration equipment must avoid refrigerant with GWP higher than 2500 by 2020, while refrigerator and freezer should employ fluid with GWP<2500. While the USA EPA erected a restriction against over 25 high GWP fluids. Commonly used R134a, R410A and R407C were deemed unacceptable in chiller systems from 2024. These policies pressured the HVAC industry into considering applying new alternative low GWP refrigerant. However, pure HFOs refrigerants have been reported to have poorer heat transfer coefficient in comparison to their predecessor. Therefore, HFO/HFC refrigerant mixture were considered as drop-in replacement as they combine the advantages of having lower GWP while maintaining heat transfer performance closer to replaced refrigerant. Among these is R448A, a recent zeotropic blend of R32 (26%), R125 (26%), R134a (21%), with HFO components R1234yf (20%) and 1234ze(E) (7%), which is a non-flammable refrigerant with a GWP of 1390 has been proposed as a low GWP alternative of R404A (GWP=3922) in direct expansion supermarket systems.

Babiloni et al (2015) experimentally evaluated R448A performance in a vapor compression system test bench and compared against the performance of R404A. Despite having lower cooling capacity than R404A, R448A had a higher COP, and was considered to be a good replacement for medium temperature application. Sethi (2016) experimentally investigated R455A and R488A performance in a commercially available R404A self-contained freezer. Compressor energy consumption of R448A was 9% lower, and R448A matched the capacity with 4 to 8% higher efficiency compared to R404A. They concluded that R448A would be a suitable replacement of R404A in

commercial refrigeration systems as well as for retrofitting. These previous result have encouraged R448A as a viable alternative refrigerant for R404A and R410A.

However, despite the potential application, the heat transfer performance of R448A inside evaporator, is still under-reported. Lillo (2019) experimentally investigated boiling heat transfer and pressure drop of R448A and compared with R404A inside a 6mm tube. They found R404A provided higher heat transfer coefficient at low vapor quality, but lower convective effect than R448A, and R448A pressure drop was always higher than R404A at the same operating condition. Kedzierski (2016) studied experimentally convective boiling inside horizontal microfin tube of 3 low GWP alternative of R448A, R449A and R452B. R454B exhibited the highest heat transfer coefficient, with R449A approximately 8% larger than R448A. As far as the authors are aware, no more paper have studied the boiling heat transfer of R448A. However, flow boiling heat transfer and pressure drop of low GWP alternative zeotropic mixture in both conventional and micro-tube has been studied extensively thank its attraction. Minxia et al (2012) experimentally investigated boiling heat transfer and pressure drop of R32/R1234yf mixture with different composition in a 2 mm diameter test tube. They found that the effect of mass diffusion resistance on heat transfer was significant, and boiling number correlates directly with the relative role of convective and nucleate boiling mechanism. Berto et al (2020) measured R455A and R452B boiling heat transfer coefficient in an 8mm and 0.96 mm tube. They discovered that R452B displayed a higher heat transfer coefficient than R455A. The heat transfer coefficient of both blend increased with heat flux, mass flux, vapor quality in the 8mm diameter channel, yet R455A heat transfer coefficient was less sensitive to mass velocity in the 0.96mm diameter channel. In addition, the 0.96mm tube has higher heat transfer coefficient than the 8mm channel. Jige et al (2020), studied flow boiling of R1234yf/R32 zeotropic mixture at 2 different circulation compositions inside multiport mini-channel tube. They observed heat transfer coefficient to be strongly influence by mass flux, quality, mass fraction, yet heat flux effect was small. Heat transfer deterioration due to mass transfer resistance was significant in nucleate boiling and in thin film evaporation, but less in annular flow regime.

In this work, the heat transfer characteristic of R448A will be experimentally investigated in a multiport mini-channel tube. The range of mass flux was from 100 kg/m²s to 500 kg/m²s, while heat flux was from 3 kW/m2 to 15 kW/m2. The corresponding inlet saturated temperature is fixed at 6°C and 3°C. The effect of heat flux, mass flux and vapor quality as well as saturated temperature on heat transfer coefficient are analyzed. The heat transfer performance between R448A was compared to the soon-phased out R410A. Finally, a new correlation was proposed for the practical prediction of R448A heat transfer coefficient.

2. EXPERIMENTAL METHOD

2.1 Experimental systems and procedure

Heat transfer coefficient and pressure drop were co-investigated in the experimental systems whose schematic was presented in Figure 1
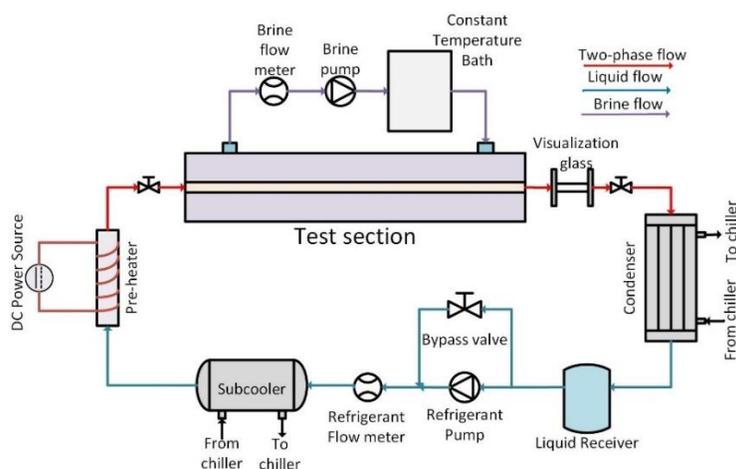

Figure 1: Experimental systems.

The systems consisted of a primary refrigerant loop and an auxiliary test section loop. Both loops were connected to a data-logger linked to a computer for monitoring and recording of the experimental data. Refrigerant post condenser in liquid phase was circulated by a magnetic micro-gear pump with adjustable frequency. A flowmeter was installed right after the pump to measure the refrigerant mass flow rate. Refrigerant might be slightly heated from the pump, and therefore a sub-cooler was installed to ensure only liquid refrigerant can enter the preheater. The preheater, a tube section with two ends connected to a controllable DC power source, heated the liquid flow to the desired testing quality before entering the test section. Two-phase refrigerant flow after the test section finally returned to be condensed back to liquid phase within the condenser. An out-of-loop chiller provided the refrigeration effect for the chilled brine, a secondary fluid which supplied the cooling capacity for the condenser and the sub-cooler.

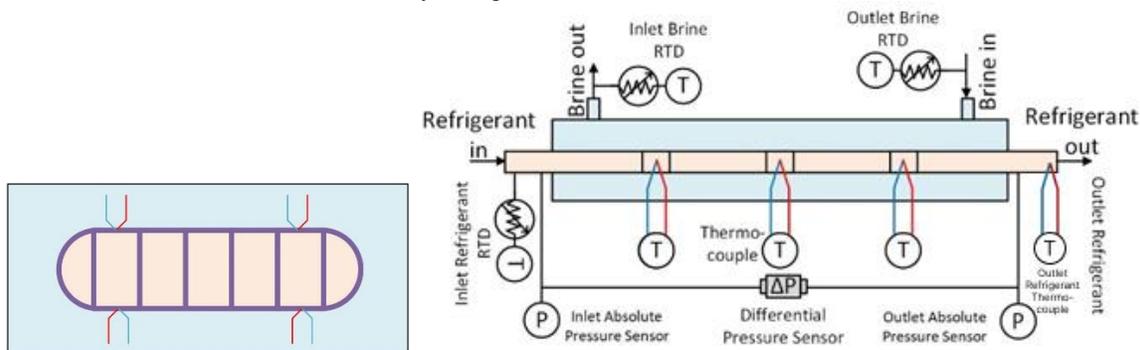The test section was described schematically in Figure 2.

Figure 2: Detail of test section.

A multiport mini-channel tube was used for the test section. The test tube was fixed in the middle of the acrylic cover, with the annuli space in between was where the warm water passed to heat the test tube. The flow directions of the refrigerant and the water jacket was counter current flow. Water temperature was controlled and kept constant to accommodate each different testing heat flux condition by a temperature bath. A pairs of RTD, calibrated to 0.01°C accuracy, was installed at the inlet and the outlet of the water path to measure the inlet/outlet temperature. Additionally, a mass flowmeter was used to measure the water flow rate. In order to calculate the heat transfer coefficient, 12 thermo-couples were embedded onto the test tube outer surface (in 3 different position, 4 in each position with 2 on top and 2 at the bottom of the tube). The junction was fixed by covering it with aluminum tape. To avoid measurement bias from leaving the thermocouple junction exposed to the water, a layer of glue was applied on top of the junction on the tape. The inlet temperature and pressure were measured with a RTD sensor and an absolute pressure transducer for the determination of the inlet vapor quality. A differential pressure sensor was installed at the test section inlet and outlet to facilitate the measurement of pressure drop. The outlet temperature thermocouple was installed to compare the measured temperature to the calculated temperature, to make sure the heat balance, pressure drop and saturated temperature calculation were correct. The deviation between the measured and calculated outlet temperature fell mostly under the combined uncertainty of the measurement and calculation, which was 0.15°C.

A data point was continuously measured in 10 minutes and averaged. Before each measuring session, the pump speed, preheater's power source, supplied brine temperature, heating water temperature and pumping speed were controlled simultaneously to establish the required testing condition. The system pressure was controlled by adjusting the temperature of the out-of-loop supply chilled brine, while the inlet temperature was controlled primary with the DC power supplied to the pre-heater. The system was then kept until a relative stability is achieved before recording.

The geometrical configuration data of the test tube is provided in Table 1 while the experimental conditions are summarized in Table 2

Table 1: Test tube geometrical configuration.

Hydraulic diameter	Length	Aspect ratio	Number of ports	Wall Thickness
0.969 mm	0.2 m	0.49	9	0.34 mm

2589, **Page 4**

Table 2: Experimental condition.

Refrigerant	Saturated temperature	Quality	Mass flux	Heat flux
R448A	6ºC and 3ºC	0 to 1 (5-6 different qualities)	100 to 500 kg/m²s	3 to 15 kW/m²

2.2 Data Reduction

The data reduction was performed consequently as follows. The heat flux applied to the test section can be calculated as. This equation assume that heat flux was constant across the tube, this assumption is reasonable as the variation of water and refrigerant temperature:

$$q = \frac{m_{water} C_{p_{water}} (T_{water,in} - T_{water,out})}{A_{ext}}$$ (1)

Unlike pure fluid, R448A is a zeotropic mixture with a large temperature glide (roughly 6ºC). This characteristic was taken advantage of to determine the refrigerant inlet enthalpy:

(2)
$$i_{in} = f(T_{in}, P_{in})$$

Assuming the applied heat flux to be constant, the enthalpy of the ith measurement point can be calculated as:

(3)
$$i_i = i_{in} + \frac{qP}{m_{ref}} z_i$$

As commonly employed within literature, the pressure of the ith measurement point was calculated by assuming the pressure drop to be linear across the tube. The current assumption is reasonable because acceleration pressure drop was small when comparing to measured pressure drop under most cases, as well the small variation of quality across the test section:

$$P_i = P_{in} - \Delta P \frac{z_i}{L}$$ (4)

The refrigerant saturated temperature of that point was determined as:
$$T_{sat_i} = f(i_i, P_i)$$ (5)

Under a low mass flux condition, the increase of saturated temperature was caused primary by changing of quality, while at a high mass flux condition, the saturated temperature decreased with decreasing pressure due to large frictional pressure gradient.

Finally, the heat transfer coefficient was calculated by:
$$h_i = \frac{A_{ext}}{A_{in}} \frac{q}{T_w - T_{sat_i}}$$ (6)

The reported heat transfer coefficient was the averaged value of all 12 thermocouples.

2.3 Uncertainty Analysis

The uncertainty analysis was performed according to ISO 1995 guideline, in which, uncertainty of a measurement was composed of 2 types of uncertainty. Type B uncertainty, the uncertainty of the instrument, was specified by the manufacturers. Type A uncertainty, based on statistical analysis, takes into account random error (fluctuation) that occurred during experiment. As such, system was set to remain as stable as possible in order to reduce type A uncertainty. Type A uncertainty was taken as the standard deviation of the mean of the measurement interval:

$$s^2(\bar{q}) = \frac{s^2(q_k)}{n} = \frac{1}{n(n-1)} \sum_1^n (q_j - \bar{q})^2$$ (7)

For parameters that was not directly measured, their errors have to be determined through the method of error propagation.

$$u_c^2(y) = \sum_1^N \left(\frac{\partial f}{\partial x_i}\right)^2 u^2(x_i)$$ (8)

For parameters that do not have explicit functional form as in equation (1), (2) and (5), their error was estimated numerically with central finite differentiation (as suggested by Moffat, 1988):

$$u_c^2(y) = \sum_1^N \left(\frac{f(x_i + u(x_i)) - f(x - u(x_i))}{2u(x_i)} \right)^2 u^2(x_i) \tag{9}$$

The uncertainty of heat transfer coefficient varied by conditions. The high mass flux condition usually had moderate to small uncertainty, within a range of about under 12% or up to under 22%. Data points with the highest experimental uncertainty were high mass, low heat flux data points, where the maximum uncertainty could reach over to 40%, as in these conditions still had a high heat transfer coefficient despite having low heat flux, causing the temperature difference to be small; hence, the large experimental uncertainty.

3. RESULT AND DISCUSSION

3.1 Mass flux, heat flux and vapor quality effect

The mechanism of flow boiling can be de-composed to 2 mechanisms: nucleate boiling and convective boiling. In this section, the data will be analyzed through this lens.
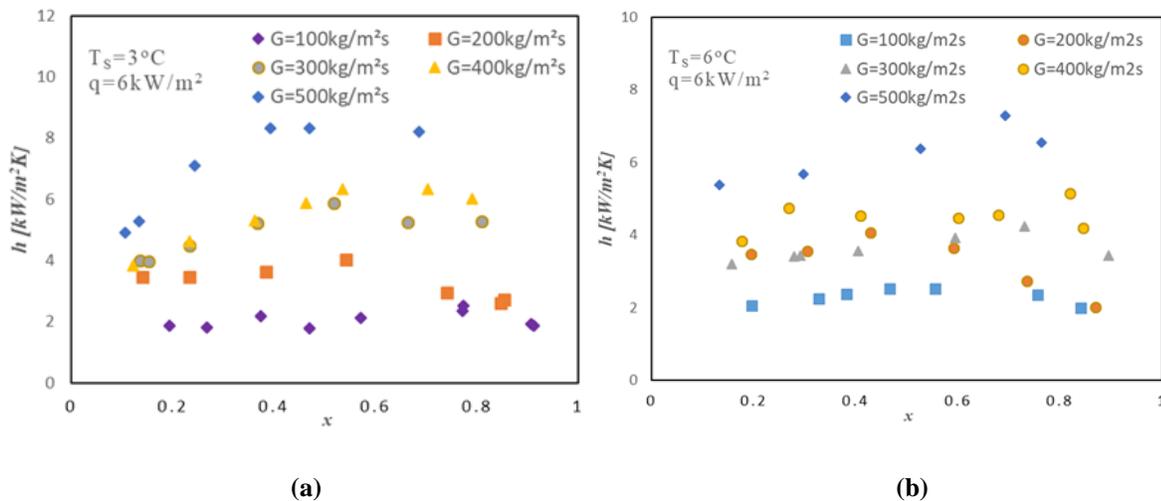

(a)	**(b)**

Figure 3: The effect of mass flux on heat transfer coefficient at two different saturated temperature of (a) 3°C and (b) 6°C

In Figure 3a and 3b, the effect of mass flux on heat transfer coefficient was illustrated at two different saturated temperatures at the fixed heat flux of 6kW/m². As shown, mass flux increased the heat transfer coefficient. At the saturated temperature of 6°C, mass flux increased the value of the heat transfer coefficient in low quality region, while at the saturated temperature of 3°C, mass flux increased both the aforementioned value, as well the increase rate of heat transfer coefficient against quality. Two distinct mechanisms brought about this effect, which were interfacial shear stress and turbulent effective conductivity. The higher the mass flux, the higher the Reynolds number, which is associated with high turbulence intensity, promoting higher effective turbulence thermal conductivity. Increasing the mass flux also increases the liquid/vapor relative velocity, as can be shown through the following equation:

$$\Delta v_{lv} = v_v - v_l = G \left(\frac{x}{\rho_v \alpha} - \frac{1-x}{\rho_l (1-\alpha)} \right) \tag{10}$$

As mass flux has little influence on void fraction α, the relative velocity Δv will increase with G. High relative velocity positive enhanced the interfacial shear stress and promote the thin film evaporation, which are beneficial for heat transfer due to flow pattern development. As decreasing saturated temperature increase the liquid/vapor density ratio (from 42.2 at 6°C to 46.8 at 3°C), the relative velocity, and with it the interfacial shear stress therefore increases more rapidly with quality. Thus explaining the more rapid increase of the heat transfer coefficient with quality at saturated temperature of 3°C when compared to 6°C.
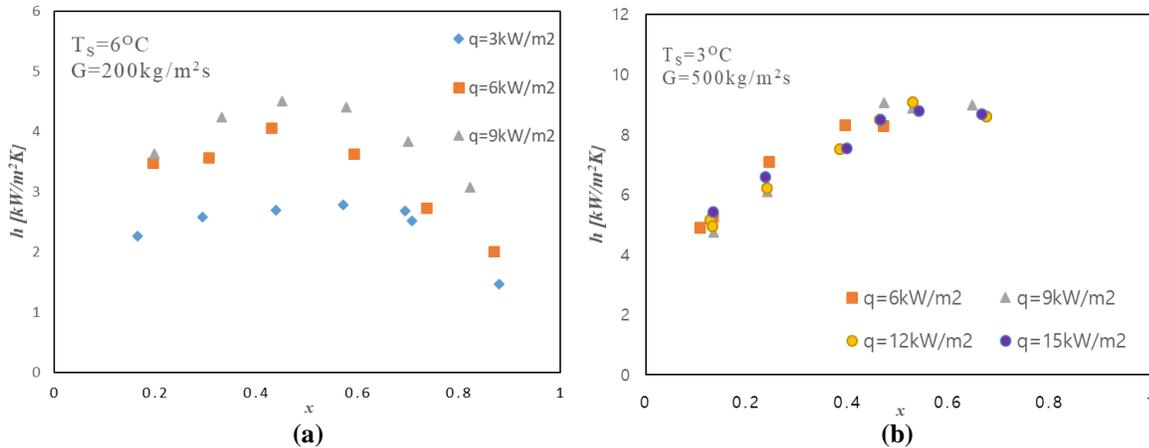
Figure 4: The effect of heat flux on heat transfer coefficient at (a) 200kg/m²s mass flux and (b) 500kg/m²s mass flux condition.

Figure 4(a) and (b) displayed the effect of heat flux on heat transfer coefficient in different heat flux condition. At 200kg/m²s (4a), heat flux had a significant effect on the heat transfer coefficient, as increasing the heat flux is known to increase the number of active nucleation sites, as well as the rate of bubble growth (the well-known Cooper correlation for nucleate boiling has an explicit heat flux term). In these conditions, the nucleate boiling mechanism was in dominant over convective boiling. However, with further increase in heat flux, the enhancement was sub-sized. As according to Minxia et al. (2012), high heat flux at low mass flux condition (high Bo flow) generates vigorous bubbles, causing the concentration to be highly inhomogeneous, thus restricting the growth of heat transfer coefficient with heat flux. Higher mass flux at 500kg/m²s (4b) displays insignificant effect of heat flux on heat transfer coefficient as data point was almost lumped together. There the nucleate boiling mechanism was strongly suppressed by the strong convection effect owning to high mass flux.

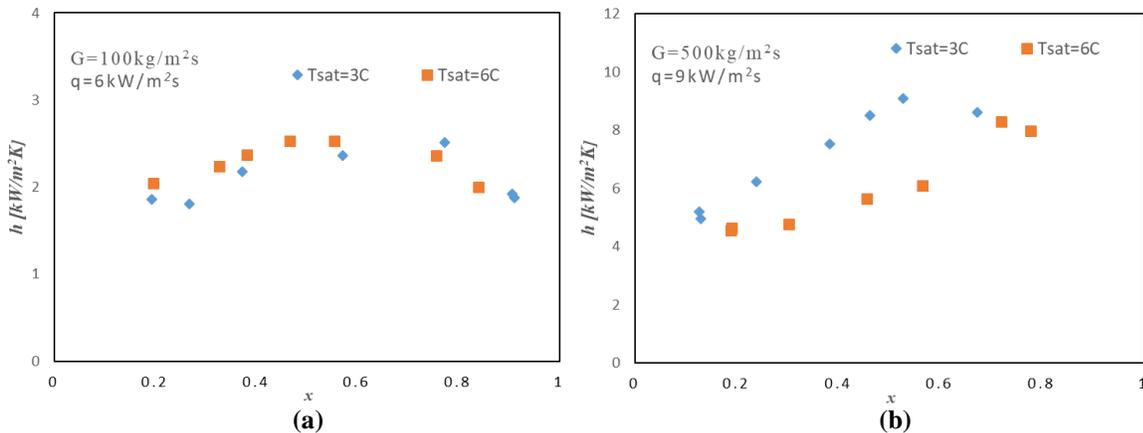## 3.2 Saturated temperature effect

Figure 5: The effect of saturated temperature on heat transfer coefficient at (a) low mass flux condition and (b) high mass flux condition.

Figure (5a) and (5b) compared the HTC of R448A at saturated temperature at 3 and 6°C. At low mass flux condition, when the nucleate boiling mechanism was dominant, the effect of saturated temperature on heat transfer coefficient was minimal. At the high mass flux condition however, the effect of saturated temperature on heat transfer coefficient was more evident. The heat transfer coefficient at a saturated temperature of 3oC is higher than at 6oC due to the larger h/x slope. At lower saturated temperature, the flow has lower reduced pressure, lower vapor/liquid density ratio and vapor density. Lower vapor density increased vapor phase velocity, while the density ratio change further increases the interphase relative velocity, boosting liquid film evaporation mechanism. As discussed, under high mass flux condition, the effect of convective boiling has a dominant role, therefore, these properties have a more significant effect on heat transfer.

3.3 Performance comparison against R410A performance

Figure 6 compared the heat transfer coefficient of R448A against R410A data at low mass flux and high mass flux conditions. The R410A data was from a previous publication by Chien et al (2018), which was performed on the same test tube.
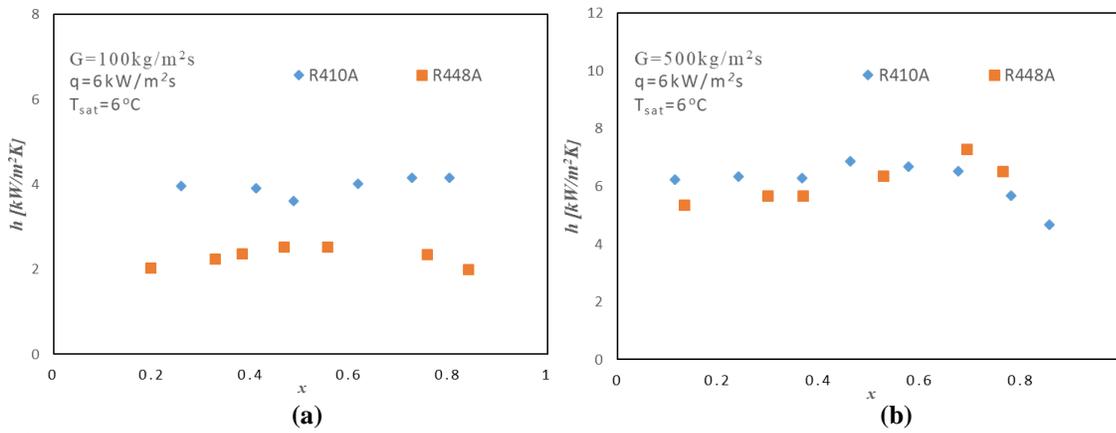

Figure 6: Heat transfer comparison of R448A against R410A in low mass flux (a) and high mass flux condition (b).

Comparing against data of for R410A, at the low mass flux condition, the heat transfer coefficient of R410A exceeded that of R448A by a considerable margin. It might be due to the fact that in mixture, during nucleation, the more volatile components were the 1st first to nucleate into the bubbles. Therefore, the vapor bubbles were rich with more volatile components, while in liquid, their concentrations were poor. This created a mass transfer barrier the more volatile components must overcome to be evaporated, which subdued the bubble growth rate and heat transfer coefficient. As R448A is a zeotropic mixture with considerable temperature glide, the mass transfer resistance during nucleate boiling was severe, when comparing to R410A, which is a near zeotropic mixture with negligible temperature glide and small mass transfer resistance. With increasing mass flux, the heat transfer increases with increasing mass flux, and mass transfer resistance due to concentration still exists at the interface; however, the strong turbulence effect produces better mixing and partly counteracted the effect of concentration in im-homogeneousity. Yet, despite having higher liquid/vapor density ratio, R448A the heat transfer coefficient of R448A can only be in a similar order of magnitude when compared with R410A, suggesting mass transfer resistance have has a significant effect on the heat transfer coefficient

3.4 Heat transfer coefficient correlation

In this section, a simple correlation is proposed for the practical prediction of the heat transfer coefficient, Correlations that were originally developed from single component flow boiling data would become obsolete when predicting mixture flow boiling, because the complication arisen from mass transfer resistance of multi-components fluid had not been taken into account. Therefore, Shah (2015) proposed a simple method of correcting the classical heat transfer correlation so that it can be suitable for the prediction of multi-component flow boiling:

$$h_{mix} = \left[(F_{TS}Sh_{nb})^n + \left(\frac{1}{Eh_l} + \frac{Y}{h_v} \right)^{-n} \right]^{\frac{1}{n}} \tag{11}$$

The nucleate boiling heat transfer contribution (right side 1st term of (11)) was modified to include the Thome and Shakir (1987) analytical factor of mass transfer resistance during the bubble nucleation.

$$F_{TS} = \left(1 + \frac{h_{nb}\Delta T_{gl}}{q} \left[1 - \exp\left(-\frac{Bq}{\rho_l \Delta h \beta_l} \right) \right] \right)^{-1} \tag{12}$$

The convective boiling contribution (right side 2nd term of (11)) was also modified to include Bell-Ghaly (1973) term to take into account the effect of mass transfer resistance at the interface. The Y term can be calculated as:

$$Y \approx xC_{pv}\frac{\Delta T_{gl}}{\Delta h} \tag{13}$$

The heat transfer coefficient was compared against 3 different heat transfer models originally developed from single component data, but modified according to the Shah (2015) model: Liu-Winterton (1997), Bertsh (2009) and Steiner & Taborek (1992). The result was shown in Table 4, and as it is shown, none of the three model gave an satisfactory

prediction. Therefore, a new simple correlation was proposed with the using the method of Shah (equation (11)). An exponential of 1.7 was used to allow for a smoother transition from nucleate boiling to convective boiling:

$$h_{mix} = \left[(F_{TS} h_{nb})^{1.7} + \left(\frac{1}{E h_l} + \frac{Y}{h_v} \right)^{-1.7} \right]^{\frac{1}{1.7}} \tag{14}$$

The nucleate boiling heat transfer coefficient was calculated by the well-regarded equation of Cooper (1984), while the convective boiling was by the Dittius-Boelter with single phase liquid.

The enhancement factor of convective boiling was found to be very well correlated with the Lockhart-Martinelli parameter:

$$E = 3.3461/X_{tt}^{0.526} \tag{14}$$

The remaining term followed the Shah (2015) model as previously discussed

The correlation gave a satisfactory prediction with the mean absolute deviation of 13.7% and mean signed deviation of 2.4%

Table 4: Correlation performance.

Correlation	Liu-Winterton	Bertsch	Steiner & Taborek	New correlation
Mean Absolute Deviation	38.3%	49%	64%	13.7%
Mean Sign Deviation	-38%	-47%	-64%	2.4%

3.5 Effect of mass flux, heat flux and vapor quality on R448A pressure gradient

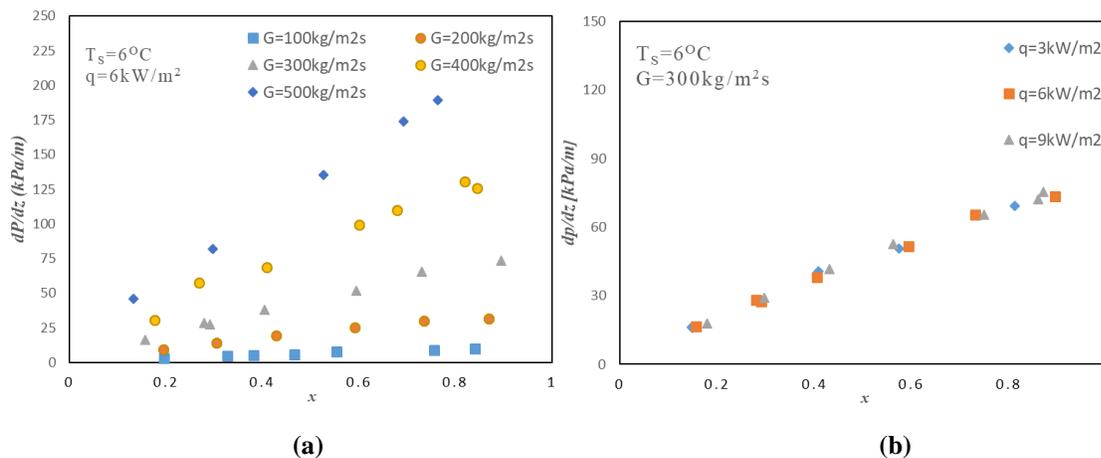Figure 7 displays the effect of heat flux and mass flux on pressure drop

(a) (b)

Figure 7: The effect of mass flux (a) and heat flux (b) on pressure drop.

As shown in Figure 7, pressure drop increased significantly with mass flux as well as with vapor quality. Mass flux increased the pressure drop at low quality as well as the pressure drop increase rate with quality. The higher the mass flux, the more intense the turbulent effect, similar to single phase flow. In addition, from equation (10), the relative liquid/vapor velocity increase with mass flux and with it the interfacial shear stress. The combined effect of turbulent shear stress and interfacial shear stress together increase the pressure drop. However, in Figure 7(b), heat flux displayed almost no effect on pressure drop, possibly because heat flux does not have an explicit influence on interfacial and turbulent shear stress

4. CONCLUSIONS

In this work, boiling heat transfer of R448A was experimentally investigated inside a multiport mini-channel tube. The effects of heat flux, mass flux, vapor quality were analyzed. The key findings are summarized as follows:

- The heat transfer coefficient always increased with mass flux. Under low mass flux condition, heat transfer coefficient increased significantly with heat flux, however in high mass flux conditions, the effect of heat

flux was found to be insignificant. Similarly, the effect of saturated temperature was significant in high mass flux condition and much less noticeable in low mass flux condition

- A comparison of heat transfer performance between R448A and R410A was done and it was found that R410A heat transfer coefficient exceed R410A's in low mass flux condition, while they are quite similar in high mass flux conditions.
- A new simple correlation was proposed following the method of Shah (2015) for the prediction of R448A boiling heat transfer coefficient inside multiport mini-channel tube. The correlation had an acceptable prediction with a mean absolute of 13.7%
- Pressure drop of R448A increase with mass flux and vapor quality, while heat flux displayed no noticeable effect.

NOMENCLATURE

i	Enthalpy	(kJ/kg)
q	heat flux	(kW/m^2)
G	mass flux	(kg/m^{2}s)
T	Temperature	(ºC)
F_{TS}	Thome-Shakir factor	
Y	Bell-Ghaly term	
X_{tt}	Lockhart-Martinelli parameter	
P	Pressure	(kPa)
m	Mass flow rate	(kg/s)
z	Length from the inlet	(m)
h	Heat transfer coefficient	(kW/m^{2}K)
A	Area	(m^2)
s	Standard deviation	
u	Uncertainty	
Subscript		
water	Water	
ref	Refrigerant	
nb	Nucleate Boiling	
cb	Convective Boiling	
in	Inlet	
out	Outlet	
sat	Saturated	
int	Internal	
ext	External	

REFERENCES

Azzolin, M., Bortolin, S., Del Col, D., (2016), Flow boiling heat transfer of a zeotropic binary mixture of new refrigerants inside a single microchannel, International Journal of Thermal Sciences, Volume 110, Pages 83-95,

Babiloni, A., Esbri, J., Peris, B., Moles, F., Verdu, G. (2015)., Experimental evaluation of R448A as R404A lower-GWP alternative in refrigeration systems, Energy Conversion and Management, Volume 105, Pages 756-762, ISSN 0196-8904.

Bell, K.J, Ghaly M.A (1973), An approximate generalized design method for multicomponent/partial condensers, AIChE Symp. Ser., 69, pp. 72-79.

Berto, A., Azzolin, M., Bortolin, S., Guzzardi, C., Del Col, D., (2020), Measurements and modelling of R455A and R452B flow boiling heat transfer inside channels, International Journal of Refrigeration, Volume 120, Pages 271-284.

Bertsch, S.S, Groll, E.A., Garimella, S.V (2009),A composite heat transfer correlation for saturated flow boiling in small channels, Int. J. Heat Mass Transfer, 52 (2009), pp. 2110-2118.

Chien., N.B, Choi, K-I., Oh J.T., Cho, G. (2018), An experimental investigation of flow boiling heat transfer coefficient and pressure drop of R410A in various minichannel multiport tubes, International Journal of Heat and Mass Transfer, Volume 127, Part A, Pages 675-686, ISSN 0017-9310.

Chiou, C.B., Lu, D.C., Liao C.Y., Su, Y.Y. (2009). Experimental study of forced convective boiling for non-azeotropic refrigerant mixtures R-22/R-124 in horizontal smooth tube, Applied Thermal Engineering, Volume 29, Issues 8–9, 2009, Pages 1864-1871.

Cooper, M.G. (1984), Heat flow rates in saturated nucleate pool boiling–A wide-ranging examination using reduced properties, Adv. Heat Transf., 16, pp. 157-239

Dang C., Jia, L., Peng, Q., Yin, L., Qi, Z. (2018), Experimental study on flow boiling heat transfer for pure and zeotropic refrigerants in multi-microchannels with segmented configurations, International Journal of Heat and Mass Transfer, Volume 127, Part C, Pages 758-768, ISSN 0017-9310.

Dang, C., Jia, L., Zhang, X., Huang, Q., Xu, M. (2017), Experimental investigation on flow boiling characteristics of zeotropic binary mixtures (R134a/R245fa) in a rectangular micro-channel, International Journal of Heat and Mass Transfer, Volume 115, Part A, Pages 782-794, ISSN 0017-9310.

Deng, Q., Zhang, Z., Hu, X., Thermoeconomic and environmental analysis of an inverter cold storage unit charged R448A, Sustainable Energy Technologies and Assessments, Volume 45, 101159,

European Parliament and the Council of the European Union. Directive 2006/40EC of the European Parliament and of the Council of 17 May 2006 relating to emissions from air conditioning systems in motor vehicles and amending Council Directive 70/156/EC, Off. J. Eurp. Union, col. 161, 2006, pp. 1–11.

Jige, D., Kikuchi, S., Mikajiri, N., Inonue, B. (2020), Flow boiling heat transfer of zeotropic mixture R1234yf/R32 inside a horizontal multiport tube, International Journal of Refrigeration, Volume 119, Pages 390-400, ISSN 0140-7007.

Kedzierski, M.A & Kang, D. (2016), Horizontal convective boiling of R448A, R449A, and R452B within a micro-fin tube, Science and Technology for the Built Environment, 22:8, 1090-1103.

Kondou, C., BaBa, D., Mishima, F., Koyama, S. (2013), Flow boiling of non-azeotropic mixture R32/R1234ze(E) in horizontal microfin tubes, International Journal of Refrigeration, Volume 36, Issue 8, Pages 2366-2378.

Li, M., Chaobin. D. & Hihara. E. (2012). Flow boiling heat transfer of HFO1234yf and R32 refrigerant mixtures in a smooth horizontal tube: Part I. Experimental investigation, International Journal of Heat and Mass Transfer, Volume 55, Issues 13–14, Pages 3437-3446.

Lillo, G., Mastrullo, R., Mauro, A.W., Pelella, F., Viscito, K. (2019) Experimental thermal and hydraulic characterization of R448A and comparison with R404A during flow boiling, Applied Thermal Engineering, Volume 161, 114146, ISSN 1359-4311.

Liu, Z., Winterton, R.H.S (1991) ,A general correlation for saturated and subcooled flow boiling in tubes and annuli, based on a nucleate pool boiling equation, Int. J. Heat Mass Transfer, 34 (1991), pp. 2759-2766

Mastrullo, R., Mauro, A.W., Viscito, l. (2019), Flow boiling of R452A: Heat transfer data, dry-out characteristics and a correlation, Experimental Thermal and Fluid Science, Volume 105, Pages 247-260.

Shah, M.M (2015), A method for predicting heat transfer during boiling of mixtures in plain tubes, Appl. Therm. Eng., 89 (2015), pp. 812-821.

Sithi, A., Pottker, G. & Motta, S.Y. (2016), Experimental evaluation and field trial of low global warming potential R404A replacements for commercial refrigeration, Science and Technology for the Built Environment, 22:8, 1175-1184.

Steiner D., Taborek, J. (1992), Flow boiling heat transfer in vertical tubes correlated by an asymptotic model ,Heat Transfer Eng, 13 (1992), pp. 43-69

Thome, J.R, Shakir, S. (1987), New correlation for nucleate pool boiling of aqueous mixtures, AIChE Symp. Ser., 83 (1987), pp. 46-51

Xu. J., Wang, Y., Yang, R., Liu, W., Wu, H., Ding, Y., Li, Y. (2021), A review of boiling heat transfer characteristics in binary mixtures, International Journal of Heat and Mass Transfer, Volume 164, 120570, ISSN 0017-9310.

Yang, Z., Feng, B., Ma, H., Zhang, L., Duan, C., Liu, B., Zhang, Y., Chen, S., Yang, Z., Analysis of lower GWP and flammable alternative refrigerants, International Journal of Refrigeration, Volume 126, Pages 12-22, ISSN 0140-7007.

ACKNOWLEDGEMENT